Probabilistic Seismic Hazard Assessment of Itanagar, Arunachal Pradesh, India: Insights into Tectonic Activity, Risk Zones, and Hazard Mapping

Aditya Kumar Anshu[1], Jumrik Taipodia[2*], Shiv Shankar Kumar[3] and Arindam Dey[4]

Aditya Kumar Anshu

Research Scholar, Department of Civil Engineering, National Institute of Technology Arunachal Pradesh, Itanagar 791113, India. ORCID No.: 0000-0002-9493-0166

Email: adityaanshu12345@gmail.com

Jumrik Taipodia

Assistant Professor, Department of Civil Engineering, National Institute of Technology Arunachal Pradesh, Itanagar 791113, India. ORCID No.:0000-0001-8943-8014; Email: jtaipodia@gmail.com

Shiv Shankar Kumar

Assistant Professor, Department of Civil Engineering, National Institute of Technology Patna, Bihar 800005, India. ORCID No.: 0000-0002-1751-8020; Email: k.shiv.ce@nitp.ac.in

Arindam Dey

Associate Professor, Department of Civil Engineering, Indian Institute of Technology Guwahati, Assam 781039, India. ORCID No.:0000-0001-7007-2729; Email: arindam.dey@iitg.ac.in

*Corresponding Authors **Jumrik Taipodia**
Assistant Professor
Department of Civil Engineering,
National Institute of Technology, Jote
Arunachal Pradesh, 791113, India.
Email: jtaipodia@gmail.com

Probabilistic Seismic Hazard Assessment of Itanagar, Arunachal Pradesh, India: Insights into Tectonic Activity, Risk Zones, and Hazard Mapping

Abstract

The paper presents a probabilistic assessment of seismic hazards for the Itanagar region of Arunachal Pradesh, India. In this study, earthquake data is compiled from the United States Geological Survey (USGS) around Itanagar in a circular enclosure of 500 km radius. The catalog is homogenized into a unified scale of moment magnitude. The earthquake data is collected between 1900 and 2024. The Seismotectonic Atlas (SEISAT) provided fault information, which is combined with earthquake information to facilitate detailed analysis and visualization using ArcGIS software. There are 33 active tectonic features in the study area, of which 18 are found to be potential sources of seismic activity. The Gutenberg–Richter (G–R) relationship is used to determine the seismicity parameters for each source zone. The region is divided into four primary subzones based on seismic activity and tectonic characteristics. Based on linear sources identified within and around the study area, this study estimates the seismic hazard of the region. Based on the Probabilistic Seismic Hazard Analysis (PSHA) method, peak ground acceleration (PGA) values indicate a 2% probability of exceeding 0.22g and a 10% probability of exceeding 0.36g over 50 years. A spectral acceleration (S_a) is also assessed for return intervals of 475 years and 2475 years, across 0.1 s 0.3 s, 0.5 s, 1.0 s, 2.0 s, and 3.0 s. The findings from the study are compared with the with other localities in the Northeast region, as well as with specifications outlined in the IS 1893-Part-1 (2016). The results of this study can be used to develop risk reduction strategies, risk acceptance criteria, and financial analyses based on the results of the comprehensive analysis and higher resolution hazard mapping.

Keywords: Seismic hazard analysis; Earthquake catalogue; Completeness analysis; Peak horizontal acceleration; Spectral acceleration.

1. Introduction

Large earthquakes over the years (such as 1964 Nigatta earthquake, 1897 Assam earthquake, 1934 Bihar-Nepal earthquake, 1950 Assam earthquake, 1988 Bihar-Nepal earthquake, 1989 Loma Prieta earthquake, 1995 Japan earthquake, 1999 Chi-Chi earthquake, 2010 Chile earthquake, 2011 Japan earthquake, 2015 Nepal earthquake, and 2023 Turkey earthquake) have left many lessons to ponder and understand in order to develop preventative measures and regulations to reduce the future tragedies. Since the prediction of damages or destructions caused by an earthquake in any specific area depends on several factors such as seismicity and topography of the area, type and condition of subsurface soil, groundwater and intensity of shaking, it is necessary to take the proper steps to assess the seismic hazards in order to obtain the precise estimations of seismic hazard parameters [1-6]. Apart from the aforementioned factors, some other influencing factors of seismic hazards at any particular location also account the magnitude of earthquake, duration of ground shaking, source to site distance, and the return period [7]. Therefore, the estimation of hazard analysis, considering aforementioned parameters, caused by such a large earthquake must be carried out to safe design of critical structures such as high-rise buildings, bridges and highways, which can be done either by adopting deterministic seismic hazard analysis (DSHA) and Probabilistic seismic hazard analysis (PSHA). DSHA estimates the strong ground motion parameters considering worst-case scenario earthquake, i.e., maximum credible earthquake that may severely affect the region, at a distance close to the site of interest. Since earthquake and site of interest contains several uncertainties, which is not accounted in DSHA, the estimated parameters can be best suitable for the project that does not requires great level of accuracy. Therefore, to get more accurate parameters with high level of accuracy considering probability of the occurrence of different earthquakes and the associated uncertainties, PSHA is the best option to estimate the earthquake resistant design parameters accurately [8]. Moreover, PSHA expresses the risk parameters numerically based on the correlation between the characteristics of the local seismic attenuation and the probability of occurrence. As a function of return period and fault displacement, it determines the likelihood that a site will exceed a predetermined ground motion level. Due to its ability to incorporate uncertainty, PSHA is widely used in seismic hazard studies [9].

Seismic hazard assessments across different regions of India reveal different degrees of seismic risks, as is reported by several researchers [10-24]. A seismic hazard assessment was conducted for the Himalayas and surrounding areas by Shanker and Sharma [25], focusing on the region located between 20° N - 36° N latitude and 69° E - 100° E longitude. From 1900 to 1990, earthquake data were collected from the Himalayan region and were divided into six seismogenic zones, with *b* values between 0.58 and 1.52. However, the research remained from performing the completeness study of earthquake catalog. Further, a microzonation study for Delhi region was carried out by Iyengar and Ghosh [26], with a 300 km radius centred on India Gate, using PSHA and reported PGA of 0.2g. Anbazhagan *et al*. [27] have conducted PSHA for the Bangalore region considering low-to-moderate seismic hazard zone, and the estimated PGA for this region was found to be 0.121g. This obtained PGA from PSHA is slightly lower than that obtained from DSHA; however, this is higher than the value reported in global seismic hazard maps. To refine the seismic hazard assessment, consideration of seismogenic sources within the radius of 350 km proposed by Gutenberg-Richter and Kijko-Sellevoll emphasized the importance of updating hazard maps and building codes to reflect local risks [27]. Shukla and Choudhury [28] assessed the probabilistic seismic hazard and estimated the site specific ground motions for the Kandla and Mundra ports located in the Gulf of Kachchh to decipher that the site amplification factor varied between 1.37 to 1.94. Further, to design a critical infrastructure like Kakrapar Atomic Power Station in Gujarat, a PSHA study has been performed by Mohanty and Verma [29] and PGA was found to be 0.23g considering maximum credible earthquake with notable contributions from the Narmada-Tapti and Rann of Kutch regions. This study also emphasized both maximum credible and design-basis earthquake scenarios to ensure the resilience of essential facilities. Ashish *et al*. [30] conducted a study to identify areas of high seismic risk in Peninsular India. Despite the region being characterized by a stable continental crust with moderate seismic activity, their PSHA estimated a PGA of 0.4g for a 10% exceedance probability over a 50-year period. Desai and Choudhury [31] identified the spatially varying probabilistic seismic hazard in the Mumbai region. It was deciphered that the codal provisions of IS-1893 [32], which depend on the non-probabilistic seismic hazard assessment, underestimate the potential seismic hazard of the entire Mumbai city especially the Navi Mumbai region that exhibited a significantly high probabilistic seismic hazard. To safeguard cultural heritage structures like the Gol Gumbaz in Vijayapura, South India, Patil *et al*. [33] carried out a PSHA study. The study reported PGA of 0.074g and 0.142g for 10% and 2% exceedance probabilities over a 50-year period, respectively. These findings emphasize the necessity of implementing seismic protection measures to preserve such valuable heritage sites. Shukla and Solanki [34] conducted a PSHA study for Indore city, compiling an earthquake catalog within a 400 km radius, which included the 1997 Jabalpur earthquake. The study provided hazard maps with peak ground acceleration (PGA) estimates for 10% and 2% exceedance probabilities over a 50-year period. Thus, it can be stated that region-specific seismic hazards analysis to safeguard infrastructure, cultural sites, heritage structures and communities considering all possible uncertainties associated with earthquakes and the region across India.

Northeast India is one of the most seismically active regions in the world, experiencing several large earthquakes such as the 1897 Shillong earthquake (M_w 8.1),1950 Assam earthquake (M_w 8.7), 2011 Sikkim earthquake (M_w 6.9), 2015 Nepal earthquake (M_w 7.8), 2016 Manipur Earthquake (M_w 6.7), 2017 Tripura earthquake (M_w 5.7), 2020 Mizoram earthquake (M_w 5.6), 2021 Assam earthquake (M_w 6.4), 2022 Arunachal Pradesh earthquake (M_w 5.7), 2023 Meghalaya (M_w 5.4), 2025 Manipur earthquake (M_w 5.7). Therefore, a study has been conducted for Northeast India region using PSHA by Das *et al*. [35], dividing this region into nine seismogenic source zones to capture the local variations in tectonic characteristics. This study estimates PGA and S_a values at bedrock level for return periods of 100, 225, 475, 2475, and 10000 years. The findings revealed that the seismic hazard is underestimated in some areas as per current Indian seismic code. Further, PSHA studies has been done for Tripura and Mizoram region of Northeast India by Sil *et al*. [36], covering a catalog of earthquake events dating back to 1731 within a radius of 500 km from the state boundaries, and provided seismic hazard curves, PGA, and uniform hazard spectra for the region. This study also revealed the spatial variations of peak horizontal acceleration (PHA) with probabilities of exceedance at 2% and 10% in 50 years, emphasizing the importance of updated hazard assessments in this seismically active region.

Past studies conducted by various researchers [35-37] suggested that the existing seismic hazard maps and Indian seismic codes may underestimate or inadequately capture the seismic risk in specific localized regions. For instance, Das *et al*. [35] indicated that current Indian seismic codes potentially underestimate seismic hazards in Northeastern region of India. Furthermore, previous research by Sil *et al*. [36] and Borgohain *et al*. [38] emphasized the significant spatial variability in ground motion within Northeast India, necessitating detailed local studies to ensure accurate and effective seismic hazard estimations. Consequently, this study was undertaken specifically for Itanagar, Arunachal Pradesh located in close proximity to the Himalayan plate boundary to provide region-specific seismic hazard assessment, enabling effective earthquake-resistant structural design and risk mitigation planning. Therefore, the necessity of conducting a comprehensive PSHA in Itanagar arises to address the variability in ground motion amplification due to local soil conditions along with frequency and intensity of potential earthquakes. This region consist of highly variable topography characterized by hilly terrain and river valleys, leads significant effects on seismic attenuation, which could exacerbate the impact of seismic events on structures and infrastructure. By employing PSHA framework, which integrates the inherent uncertainties associated with earthquake occurrence, ground motion prediction, and site effects, this study enables a more robust estimate of seismic hazard, providing decision-makers with critical information to develop mitigation strategies. For a rapidly developing city like Itanagar, where infrastructure projects are underway, the results of a PSHA are crucial for designing buildings and public facilities that can withstand seismic forces, thus minimizing casualties and economic losses in the event of a significant earthquake. The PSHA model for Itanagar will involve the evaluation of different seismic source zones, ground motion attenuation relationships, and local soil characteristics. This approach provides seismic hazard curves, maps of PHA, and spectral acceleration values for different return periods that will help planners and engineers to design and construct the seismically resilient structures. The present study focuses on the assessment of seismic hazard for Itanagar region in the state of Arunachal Pradesh (India) in view of planning a proposed smart city. Moreover, PHA and spectral acceleration (S_a) are used to formulate the outcomes of the seismic hazard analysis at various return periods. PHA provides insight to ground deformation, strain development, horizontal forces, and shear stresses, which are essential for earthquake-resistant design considerations; whereas, S_a represents the maximum acceleration experienced by structures represented by a single-degree-of-freedom system under damped vibrations [39]. The prepared hazard maps of Itanagar region corresponding to 475 years (10% probability of exceedance in 50 years) and 2475 years (2% probability of exceedance in 50 years) at different time periods, such as 0.1 s 0.3 s, 0.5 s, 1.0 s, 2.0 s, and 3.0 s, will help engineers and architects to plan and design of earthquake resistant structures on the highly undulated hilly terrain.

2. Study area and tectonic features

Itanagar is located in Arunachal Pradesh, which lies on the northeastern region of India, at 27°05'54"N and 93°37'19"E, as shown in Fig. 1. The entire state of Arunachal Pradesh covers an area of 83743 km^2, and is located in the Siwalik range of Himalaya, encompassing a range of elevations from 102 m to 588 m above mean sea level (MSL) [40]. It is a physiographic section of the great Himalayas, wherein Lohit, Dibang, Siang, Kameng, and Subansiri rivers are the most influencing ones among many other rivers and their tributaries. In the Himalayan Fold Thrust (HFT) belt, Itanagar lies within the active seismic domain near the plate boundary and falls under Zone-V, the highest seismic vulnerability category as per IS 1893-Part-1 [32].

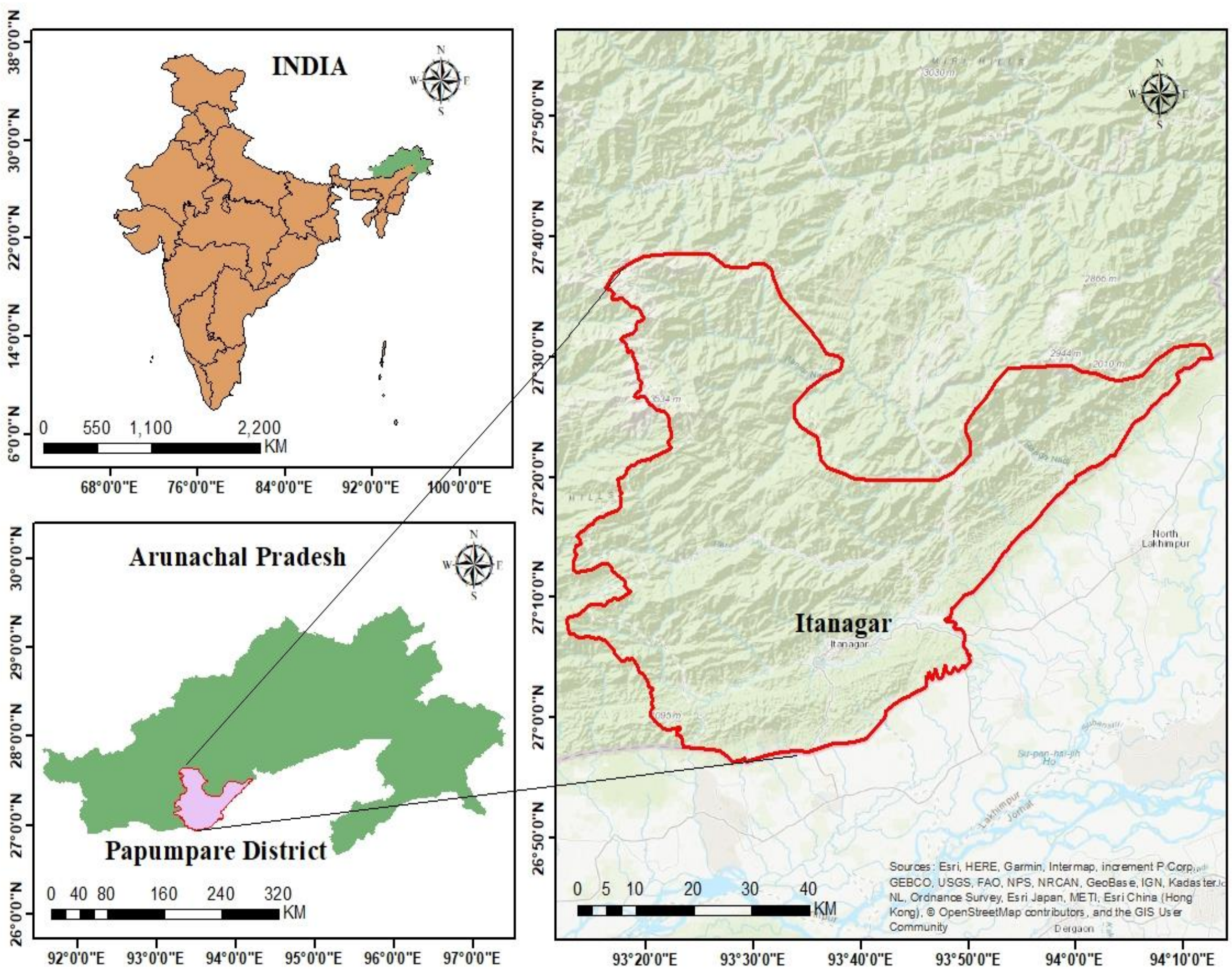

Fig. 1 Location of Itanagar in Arunachal Pradesh, India

The entire Itanagar consist of mountain slope faces, ridges and crest lines, open slopes, and mid-slope ridges with spatial extents for buildings, roads, drainage, and sewage networks. The region also consists of active seismotectonic domain surrounding the Itanagar urban agglomeration zone [41-43]. This zone is a result of collision between Indian with Eurasian plate [44,45]. Main boundary thrusts (MBT) and main central thrusts (MCT) are most likely to cause seismic events, wherein MCT reflects ductile shear zones [46]. A transverse tectonic regime throughout NE Himalayan belt is also observed with a focus depth ranging from 0 to70 km [46]. It is reported that there were two earthquakes of magnitude 7.1 and 7.8 in 1941 and 1947 in this region. The 2011

Sikkim earthquake of M_w 6.8 caused severe devastation in the Sikkim region of Northeast India. The Shillong plateau, with focal depth ranging from 0-60 km, is bordered by the Brahmaputra river fault in the north and the Dauki fault in the south. The west side consists of Dhubri fault that is oriented north-south, while the east side has the Disang thrust. Moreover, the Sylhet fault is responsible for 1918 Srimangal earthquake (M_w = 7.6). Shillong plateau is much more seismically active than Naga thrust zone. It is also called as Assam gap or aseismic corridor by the researchers [47,48]. This gap runs parallel to the Dauki fault in the south and extends parallelly to the Naga Thrust in the east. Due to the collision between Indian and Eurasian plates in Mishmi Thrust zone, seismicity of the entire region becomes significantly higher than the Eastern Himalaya [49]. As a result of the high stress concentration, this zone is classified as a special zone with block tectonics [50]. To quantify the impact of these tectonic processes and enhance our understanding of seismic patterns, the next step involves the systematic development and refinement of an earthquake catalogue for the Itanagar region.

3. Development of earthquake catalogue, homogenization and declustering

To estimate the hazards associated with earthquakes, a comprehensive earthquake catalogue is necessary. The data statistics of seismic events are essential to assess the seismic hazard of a region. The earthquake catalogue used in this study covers the earthquake period from 1900 to 2024, collected from United States Geological Survey (USGS), National Centre of Seismology (NCS) under the Government of India and International Seismological Centre (ISC). An earthquake catalogue is developed using seismic events recorded within a 500 km radius around Itanagar and includes approximately 2710 earthquake events of magnitudes exceeding 4.0 i.e., ranging from a minimum moment magnitude of 4.4 to a maximum of 8.0. This radius is selected based on established practices in seismic hazard studies for regions with complex tectonic environments and high seismic activity. Previous seismic hazard studies in Northeast India have effectively used similar radii [35, 36, 51] to adequately capture significant seismic sources influencing regional seismic hazards.

A complete and consistent earthquake catalogue is crucial for understanding seismic activity in a region. The regional earthquake catalogues are often heterogeneous due to variations in magnitude scales. Therefore, to ensure uniformity in the completeness analysis, this study converted different magnitude scales into a moment magnitude using the correlations proposed by Scordilis [52], as described in Eqns. 1-3. This standardization helps address the saturation issues associated with various magnitude scales. The catalogue includes essential information such as event coordinates, date (month and year), magnitude, and hypocentral depth.

$$M_w = 0.85\ M_b + 1.03, \text{ for } 3.5 \le M_b \le 6.2 \quad (1)$$

$$M_w = 0.67\ M_s + 2.07, \text{ for } 3.0 \le M_s \le 6.1 \quad (2)$$

$$M_w = 0.99\ M_s + 0.08, \text{ for } 6.2 \le M_s \le 8.2 \quad (3)$$

To convert local magnitude (M_L) to moment magnitude (Mw), regional correlations are typically preferred for better accuracy. For India and its surrounding regions, the correlation derived by Kolathayar *et al*. [53] is utilized, as expressed in Eqn 4.

$$M_w = 0.815 M_L + 0.767, \text{ for } 3.3 \le M_L \le 7.0 \quad (4)$$

The expressions for magnitude conversion provided by Scordilis [52] and Kolathayar *et al*. [53] are chosen based on their extensive validation for tectonically active regions and their relevance to the Himalayan and Indo-Burmese seismic zones, where Itanagar, Arunachal Pradesh, is located. Further, declustering of the homogenized catalogue is conducted to better estimate the earthquake return periods by removing foreshocks and aftershocks. Over the years, various methods have been developed globally for declustering by researchers [54–57]. In this study, declustering is conducted using a homogenized earthquake catalogue in ZMAP v2007 [58], following the algorithm proposed by Gardner and Knopoff [54]. Figure 2a illustrates the variation in seismic event depths over time, showing focal depth ranging between 10 and 120 km for most significant earthquakes in this region. Figure 2b depicts the magnitudes of seismic events over time, revealing that earthquakes with magnitudes of $M_w \le 5.0$ were only recorded after 1964, thereby hinting the absence of monitoring stations in the region prior to that period. From the initial dataset of 2710 events, 24% were identified as dependent and removed during declustering; thus, a total of 2054 mainshock event dataset is considered for further analysis. The seismic activity in the study region includes 1184 mainshocks with magnitudes between 4.0–4.9 M_w, 793 between 5.0–5.9 M_w, 64 between 6.0–6.9 M_w, 12 between 7.0–7.9 M_w, and one event is 8.0 M_w. Figure 3 presents the epicenter map of the study area, displaying all 2054 earthquake events that is included in the final catalogue.

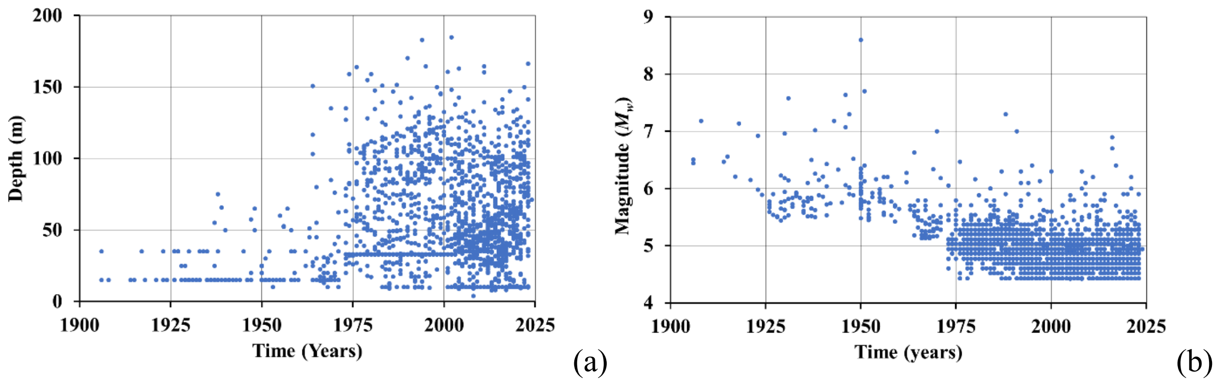

Fig. 2 Temporal distribution of declustered seismic events: (a) focal depths and (b) magnitudes, recorded between 1906 and 2024 within the influence zone of study area

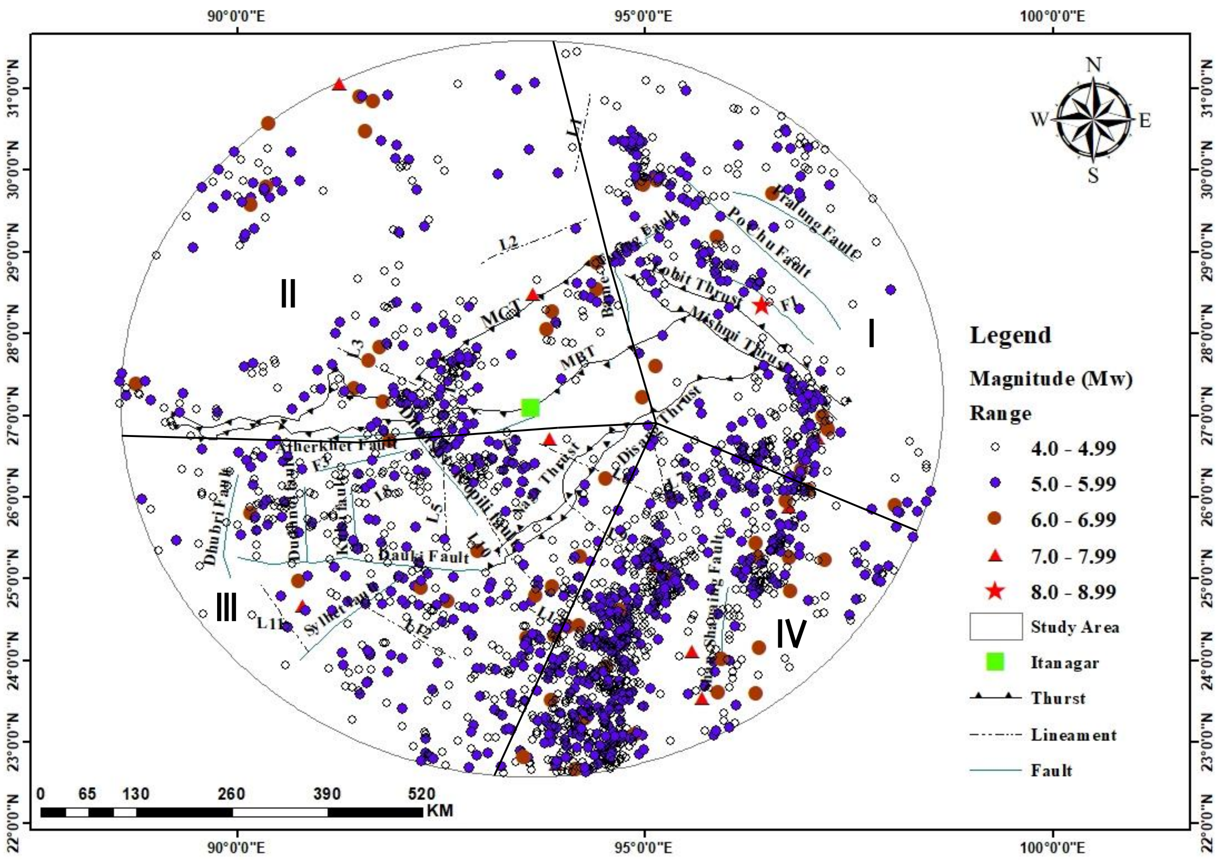

Fig. 3 Seismicity map of study area

4. Completeness of data with respect to magnitude and time

The number of earthquakes per decade is categorized into five magnitude ranges: $4 \leq M_w \leq 4.9$, $5 \leq M_w \leq 5.9$, $6 \leq M_w \leq 6.9$, $7 \leq M_w \leq 7.9$, and $8 \leq M_w \leq 8.9$. Table 1 provides a detailed count of earthquakes recorded in each decade, starting from the earliest available earthquake data. Figure 4 presents a histogram illustrating the data in Table 1 for the entire catalogue, spanning from 1906 to 2024. Developing an earthquake catalogue that encompasses a significant time period is crucial, as incomplete catalogues can lead to inaccurate estimation of seismicity parameters. To ensure completeness, the catalogue was analyzed using the Cumulative Visual Inspection (CUVI) method [59]. This method assesses completeness by plotting the cumulative number of events per year against the time of occurrence for each magnitude range. The completeness period is determined as the year from which there is a noticeable steep rise in the graph. Based on the CUVI method, the catalogue is deemed complete for large magnitude earthquakes throughout the entire time span. Table 2 demonstrates that the catalogue achieves completeness over a sufficient duration, making it reliable for seismic analysis.

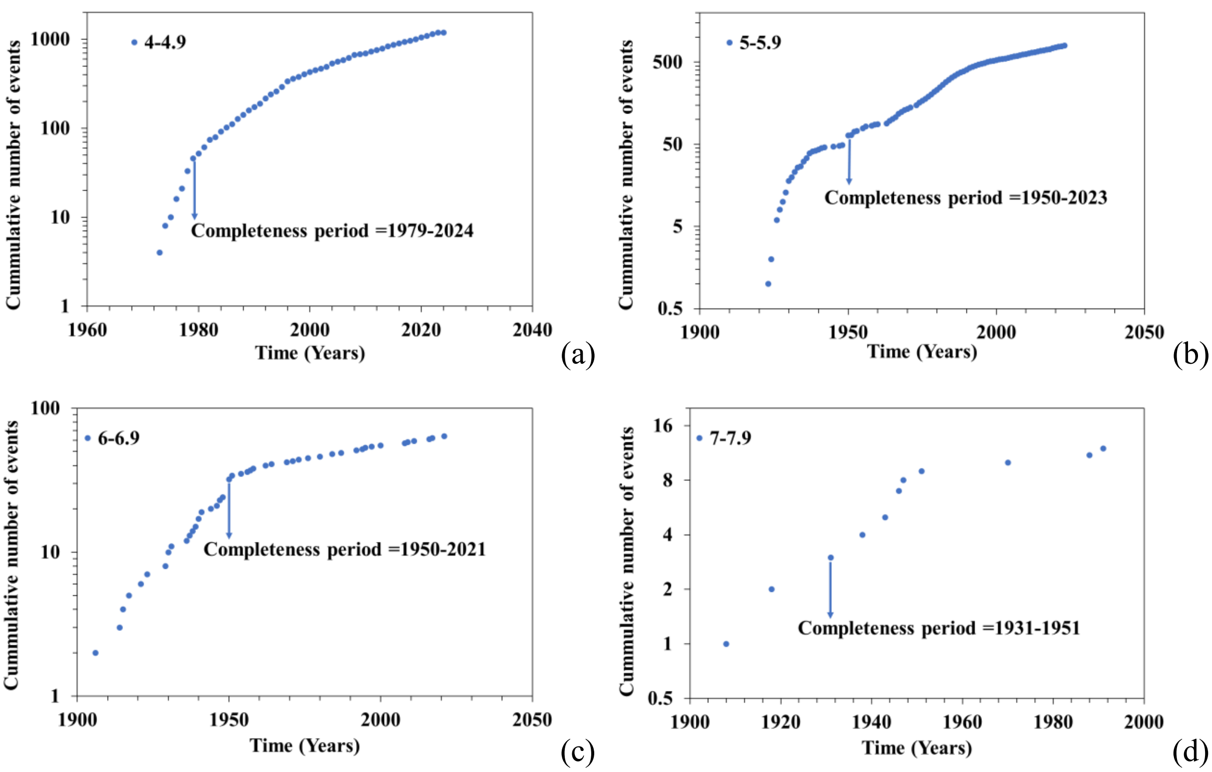

Fig. 4 Catalogue completeness by the CUVI method for the study area for various classes of earthquake magnitude

Table 1 Number of earthquakes reported in each decade for study region

Years Interval	Number of Earthquake					
	4.0-4.9	5.0-5.9	6.0-6.9	7.0-7.9	8.0-8.9	Total
1906-1915			4	1		5
1916-1925		2	3	1		6
1926-1935		29	4	1		34
1936-1945		16	9	2		27
1946-1955		31	15	4	1	51
1956-1965		24	6			30
1966-1975	10	67	3	1		81
1976-1985	92	154	4			250
1986-1995	189	155	5	2		351
1996-2005	267	98	2			367
2006-2015	307	110	4			421
2016-2024	319	107	5			431
Total	1184	793	64	12	1	2054

Table 2 Completeness analysis of earthquake catalogue

Magnitude class (M_w)	Completeness Analysis (CUVI method)	
	Period	Interval (Years)
4.0-4.9	1979-2024	45
5.0-5.9	1950-2023	73
6.0-6.9	1950-2021	71
7.0-7.9	1931-1951	20

5. Exploration and characterization of potential seismogenic sources

The process of characterizing earthquake sources includes creating tectonic maps, identifying all potential sources of damaging earthquakes, assessing the largest recorded earthquake magnitudes, measuring the lengths of faults, lineaments, and thrusts, and estimating the maximum magnitude that these seismogenic sources can generate. Measuring fault lengths is significant because it helps in understanding the size and location of potential earthquakes. By determining the dimensions of faults, researcher can assess seismic activity potential and better prepare for future earthquakes. Additionally, this information aids in assessing risk to populated areas and implementing safety measures. Estimating the magnitude potential ($M_{\max}$) of seismogenic sources is crucial for assessing the maximum magnitude of earthquakes that can occur in a given region.

5.1 Identification of seismogenic sources and development of tectonic setup

The Geological Survey of India (GSI) developed a Seismo-tectonic Atlas of India and its Environs (SEISAT) as a detailed resource for analyzing seismic activity in the area [60]. This atlas presents tectonic features and earthquake epicenters on a 1:1000000 scale across 43 sheets, each encompassing 3° longitudes and 4° latitudes. For this research, a 500 km radius surrounding Itanagar is examined using high-resolution scans of sheets 13-17. A tectonic map of the seismic study area was created by digitizing and combining these sheets, as illustrated in Fig. 4. SEISAT categorizes all linear tectonic features as either active or inactive. The distribution of seismic events across various tectonic features is revealed by overlaying recorded event epicenters on tectonic maps. This analysis showed that the seismic events occurred most frequently in zones with active tectonic features, providing valuable insights for understanding of seismic hazards in the region. In seismically active areas, there is no standardized method for identifying potential seismogenic sources [61]. Consequently, tectonic maps and historical earthquake epicenter locations are typically used as primary references in these assessments. Potential seismogenic sources are identified based on maximum observed magnitude (M_{obs}) values and their proximity to the site of interest for seismic hazard assessment. The seismic study region contains 33 active tectonic features, as shown in Fig. 4. This study considers 18 major active tectonic features capable of producing significant ground motion at the selected site for seismic hazard analysis, as listed in Table 3.

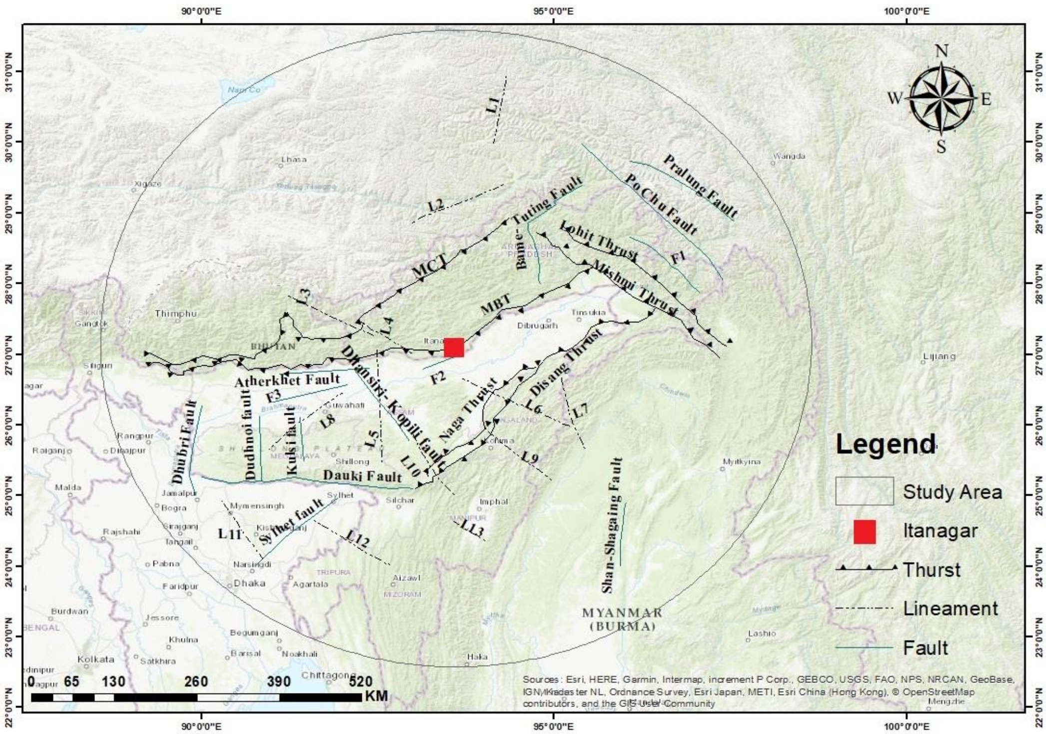

Fig. 5 Seismotectonic map showing tectonic features of the study region

5.2 Estimation of maximum magnitude potential

The maximum potential earthquake magnitude (M_{max}) plays a crucial role in seismic hazard evaluation and the earthquake-resistant design of structures. It represents the largest seismic event in an area that can be produced at a particular source. Accurate estimation of M_{max} is essential for developing effective earthquake risk reduction plans, as it directly affects the design criteria for buildings, bridges, and other vital infrastructure to endure possible seismic occurrences. Several researchers have proposed various techniques to estimate M_{max} over the time, acknowledging its significance in minimizing earthquake-related risks [62-66]. These approaches differ in their methodologies, reflecting the intricacy and variability of seismic sources across different regions. This research concentrates on the methods suggested by Gupta [63] and National Disaster Management Authority (NDMA) [66] for estimating M_{max}. Gupta [63] presented a general approach that involves adding 0.5 units to the maximum observed magnitude (M_{obs}) to determine M_{max}. This method is founded on the principle of historically maximum observed seismic magnitude that provides a baseline, which necessitates a conservative adjustment to the account of uncertainties and variations in seismic activity. In contrast, NDMA [66] approach offers a slightly different method, adjusting M_{max} on the observed magnitude. Specifically, if M_{obs} is below 5.0, a smaller increment of 0.3 is added, indicating a lower likelihood of significant magnitude escalation for smaller seismic events. Conversely, if M_{obs} is 5.0 or higher, a larger increment of 0.5 is applied, recognizing the increased probability of more substantial seismic activity in areas that have already experienced moderate to strong earthquakes. These methodologies are widely accepted and utilized because they provide a standardized, yet adaptable, approach to estimating M_{max}, ensuring that seismic hazard assessments are both realistic and conservative. These conventional and broadly adopted methods, which involve adding constant incremental values to M_{obs}, are particularly valuable for seismic sources with limited historical data, as they offer a systematic way to estimate potential maximum magnitudes in the absence of comprehensive long-term records. The application of these methods is supported by numerous studies in the field [11, 37, 67], which have demonstrated the effectiveness of these approaches in various seismically active regions.

Table 3 Estimation of M_{max} for various existing faults in the influence zone of study area

Fault Name	Total Length	M_w (observed)	Estimated M_{max}	
			Gupta [63]	NDMA [66]
MCT	700	7.3	7.8	7.8
Lohit Thurst	326	8.0	8.5	8.5
Mishmi Thurst	354	6.3	6.8	6.8
MBT	737	7.3	7.8	7.8
Naga Thurst	267	5.5	6.1	6.1
Shan-Shagaing Fault	106	7.6	8.1	8.1
Bame-Tuting Fault	209	6.4	6.9	6.9
Dhubri Fault	148	7.1	7.6	7.6
Dhansiri Kopili Fault	141	6.0	6.5	6.5
Atherkhet Fault	133	6.0	6.5	6.5
Dudhnoi Fault	106	5.5	6.1	6.1
Dauki Fault	319	7.1	7.6	7.6
Sylhet Fault	166	6.7	7.2	7.2
Pralung Fault	186	6.1	6.6	6.6
Po-Chu Fault	308	6.3	6.8	6.8
F2	60	4.9	5.4	5.2
L5	185	4.8	5.3	5.1
L6	178	6.5	7.0	7.0

6. Gutenberg- Richter seismicity parameters

The seismic study region is segmented into four distinct regions, encompassing 18 tectonic features. To estimate seismicity parameters for the region, the average observed focal depths within each seismogenic area are utilized [67]. Based on the developed earthquake catalog, the study area is divided into four regions: Region-I, Region-II, Region-III, and Region-IV, as shown in Fig. 3. According to Anbazhagan *et al*. [68], several recurrence laws describe the variability in earthquake magnitudes generated by different seismic sources, including the Gutenberg-Richter (G-R) relation [69] and the Mertz-Cornell model [70]. Among these, the G-R relation is simple and widely employed for evaluating the seismic hazard parameter, '*b*'. For conducting a Probabilistic Seismic Hazard Analysis (PSHA), the recurrence parameters '*a'* and *'b'* are critical. These parameters can be determined using the G-R recurrence law, which assumes that earthquakes occur in any given region following a Poisson distribution, implying independence in their timing and location. The Gutenberg-Richter law is expressed mathematically as follows:

$$\log \lambda_m = a - bM_w \tag{5}$$

In the Gutenberg-Richter relationship, the parameters '*a*' and '*b*' describe the seismicity of a region, while λ_m represents the average rate of exceedance for a moment magnitude M_w. The parameter '*a'* (intercept) is the logarithm of the total number of earthquakes with magnitudes equal to or exceeding the threshold magnitude. The parameter '*b'* (slope) reflects the average distribution of earthquake magnitudes in a specific area. A lower *b*-value indicates a predominance of larger magnitude earthquakes, while a higher *b*-value suggests that smaller magnitude earthquakes are more common. According to NDMA [66], the value of '*b'* varies from region to region, it lies typically in the range $0.6 < b < 1.5$. The *b*-value of the present study ranges between 0.68±0.04 to 0.89±0.03. The Gutenberg-Richter relationship for the present study area is shown in Fig. 6. Regions with lower *b*-values (e.g., Region II) are typically more prone to significant seismic hazards due to the higher frequency of large earthquakes. Regions with higher *b*-values (e.g., Region IV) are more stable with less risk of catastrophic seismic activity but experience more frequent smaller earthquakes.

The seismicity parameters (*a* and *b* values) estimated for the Itanagar region are summarized in Table 5. The *b*-value, representing the relative frequency distribution of earthquake magnitudes, is found to range from 0.64 to 0.92, aligning closely with previously reported values for seismically active regions in Northeast India, such as 0.43–1.07 by Das *et al*. [35] and 0.54–0.86 by Sil *et al*. [36]. This similarity suggests that moderate-magnitude earthquakes dominate the seismic activity in Itanagar, consistent with the regional tectonic framework. The *a*-value, which characterizes the overall seismic activity and event rate, ranges from 3.77 to 4.75 in the present study. These values correspond well to those reported from similar tectonic and seismic settings, including 4.21 for Peninsular India (Jaiswal and Sinha [71]), 3.52 for Bangalore (Anbazhagan *et al*. [27]), and a range of 2.54–4.94 for Tripura and Mizoram (Sil *et al*. [36]). Generally, higher *a*-values indicate regions with greater seismic event frequencies, thus underscoring higher overall seismic activity. The obtained *a*-values for Itanagar clearly reflect a significant level of seismic activity, confirming the need for detailed seismic hazard assessments and earthquake-resistant infrastructure design in this area.

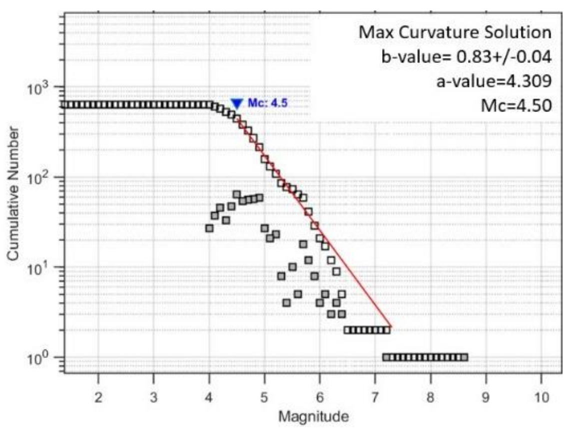

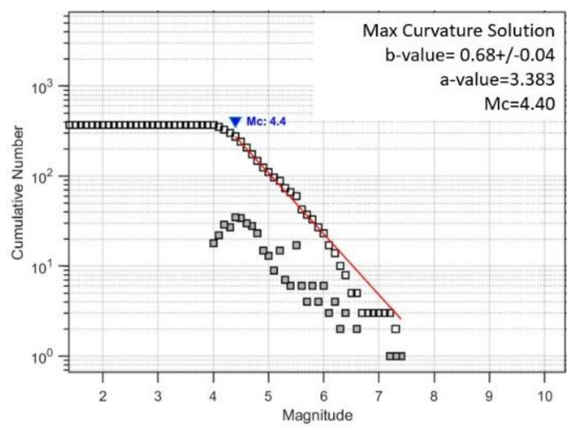

Region-I Region-II

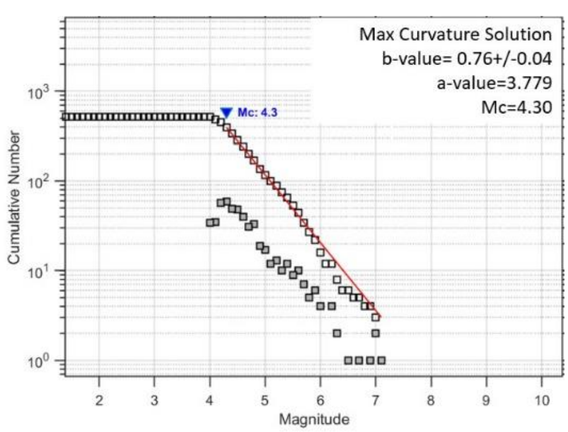

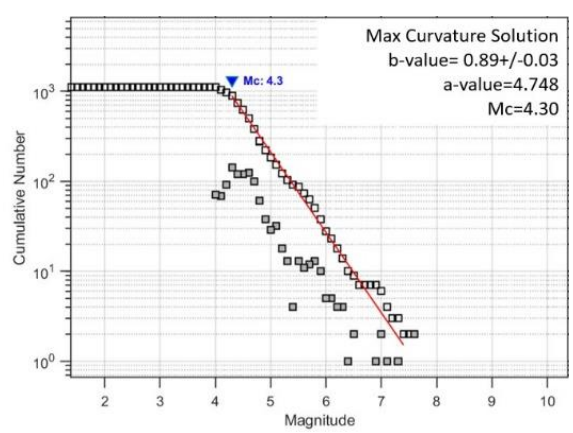

Region-III Region-IV

Fig. 6 Frequency-magnitude relationships (Gutenberg–Richter law) for four distinct regions.

Table 4. Seismicity parameters for different area sources

Region	b	a	Number of events	Range of Magnitude	Maximum M_{obs}	Return period for M_{obs} (in Years)
I	0.83±0.04	4.309	427	4.0-8.0	8.5	674
II	0.68±0.04	3.383	271	4.0-7.4	7.4	45
III	0.76±0.04	3.779	412	4.0-7.1	7.1	42
IV	0.89±0.03	4.748	923	4.0-7.6	7.6	104

Table 5. Comparison of '*b*' values obtained from present study with the previous literature.

Authors	**Study area**	***b*-value**	***a*-value**	**Data period (years)**
Ram and Rathor [70]	South India	0.81	-	70
Kaila *et al.* [73]	South India	0.7	-	14
Rao and Rao [72]	Peninsular India	0.85	4.4	170
Raghukanth and Iyenger [75]	Mumbai	0.86	0.77	-
Jaiswal and Sinha [71]	Peninsular India	0.92	4.21	160
Anbazhagan *et al.* [27]	Bangalore	0.86	3.52	200
Vipin *et al.* [76]	South India	0.891	4.58	400
Menon *et al.* [77]	Tamil Nadu	1.13	5.05	501
Sitharam *et al.* [78]	Karnataka	0.923	4.75	400
Shukla and Choudhury [79]	Gujarat	0.51	-	188
Kolathayar *et al.* [23]	India	0.5-1.5	3-10	1760
Kumar *et al.* [80]	Lucknow	0.80-0.86	3.2-4.07	170
Sil *et al.* [36]	Tripura & Mizoram	0.54-0.86	2.54-4.94	279
Naik *et al.* [81]	Goa	0.91	6.41	246
Shiuly *et al.* [82]	Kolkata	0.738	2.73	120
Das *et al.* [35]	Northeast region	0.43-1.07	1.68-5.76	113
Present study	Itanagar	0.64-0.92	3.77-4.7	124

7. Probabilistic seismic hazard analysis

The hazard analysis in this study was conducted using R-Crisis v18.2 that is a windows-based software developed by Ordaz and Salgado-Gálvez [83]. R-Crisis is specifically designed for PSHA and calculates seismic hazard by incorporating earthquake occurrence probabilities, attenuation patterns, and seismicity trends. For PSHA, the software supports three types of probable source geometries: areas, lines, and points. The analysis utilizes the earthquake catalogue for the study region in a homogenized form of the moment magnitude scale. Key seismic parameters such as maximum magnitude ($M_{\max}$), earthquake activity rate (k), and the b-value are calculated using the frequency–magnitude distribution proposed by Gutenberg and Richter [69]. One of the critical outcomes of the PSHA is the estimation of PHA, which quantifies the intensity of ground shaking during an earthquake at a specific location. This study presents a summary of PHA values for the Itanagar region for various structural periods and return periods, providing valuable insights into the seismic risk for the area.

Consequently, the development of a new Ground Motion Prediction Equation (GMPE) is not undertaken. Globally available GMPEs are reviewed to identify a suitable model for the Itanagar area, which is located in a highly seismically active region and is particularly vulnerable to shallow crustal earthquakes, similar to those in the Northeast Himalayan region [43, 84]. To select an appropriate GMPE, several models for shallow crustal earthquakes are evaluated by comparing the observed and calculated PGA values for past seismic events, including the 6.8 M_w Sikkim earthquake of 2011 and other regional events [85]. Following this analysis, the attenuation model by Boore *et al*. [86] is identified as the best-fit model for the study area, based on its superior agreement with observed seismic data. Due to limited and publicly unavailable earthquake data, it becomes even harder to deal with different types of uncertainties [87]. As a result, global models like NGA-West2 [84] are often used for seismic hazard studies in India and the Himalayan region. Previous studies, such as Sharma *et al*. [88] and Ornthammarath *et al*. [89], have demonstrated the reliability of the Boore *et al*. [84] GMPE in seismic hazard analyses for Himalayan and Indo-Burmese regions, where established local GMPEs are currently unavailable. Additionally, Ghione *et al*. [90] and Lallawmawma *et al*. [91] support the application of global GMPEs in seismic hazard assessments for Northeast India, emphasizing their suitability in estimating strong ground motions. The selection of the Boore *et al*. [86] model in this study is further justified by the similarities in tectonic stress regimes, seismogenic depths, and geological conditions between the study area and other seismically active areas where this GMPE has been validated. While the importance of developing region-specific GMPEs is acknowledged, the current absence of adequate strong-motion data from study region necessitates the adoption of a widely tested, globally validated GMPE, ensuring robust and reliable ground motion estimates. The seismic hazard is assessed for return periods of 475 years (10% probability of exceedance in 50 years) and 2475 years (2% probability of exceedance in 50 years). Using R-Crisis, which supports various verified GMPEs, the analysis generated exceedance probability plots and stochastic event simulations. The input parameters for the computational framework included seismicity constants (a, b), minimum and maximum magnitudes ($M_{\min}$, $M_{\max}$), focal depths, and the selected attenuation model. In this study, these parameters include the precise hypocentral depths, which are determined based on historical earthquake records, with average depths calculated as 35 km, 28 km, 40 km and 70 km for Regions I, II, III and IV, respectively. The software also requires the information about fault geometry and characteristics of seismic sources, for which 18 major tectonic faults (identified through the Seismotectonic Atlas SEISAT, GSI, and digitized in ArcGIS software) are modeled as line sources. The PHA values for the Itanagar region are calculated across a grid of points, and the results are represented as contour maps. For a return period of 475 years, the estimated PHA is 0.22g, corresponding to a 10% probability of exceedance in a 50year period (Fig. 7a). For a 2475year return period, the PHA increases to 0.36g, representing a 2% probability of exceedance in the same timeframe (Fig. 7b). These contour maps provide a visual representation of the seismic hazard distribution in the region.

It is noteworthy that the Indian code of practice, IS 1893-Part-1 (2016) [32], classifies the entire northeastern region of India, including the study area, as seismic zone V, assigning a PHA value of 0.36g without referencing a specific return period. In this study, the computed PHA values for return periods of 475 years and 2475 years are found to be consistent with the value recommended by IS: 1893. Specifically, the PHA values of 0.22g for a 475 year return period and 0.36g for a 2475year return period align well within the prescribed limit of 0.36g, supporting the reliability of the hazard estimates. The seismic hazard assessment for the Itanagar region, based on spectral acceleration (S_a) contours at a 475year return period across periods of 0.1 s, 0.3 s, 0.5 s, 1.0 s, 2.0 s and 3.0 s, reveals significant spatial variability in seismic intensity, have been plotted as contour map in Fig. 8(a-f).

The southern and central areas consistently exhibit higher S_a values, peaking at 0.54g for the 0.1 s period, indicating elevated seismic hazard. In contrast, the northern and western regions display lower S_a values, with a minimum of 0.024g at the 3.0 s period, suggesting reduced seismic risk. These spectral acceleration values indicate the potential severity of ground shaking during an earthquake, with higher values suggesting more intense shaking. At 0.54g for 0.1 s, the risk of structural damage is significant, especially for buildings not designed to withstand such forces. As the spectral acceleration decreases with longer periods, the risk for taller structures or those with longer natural periods may still be considerable if they are not adequately engineered for these conditions.

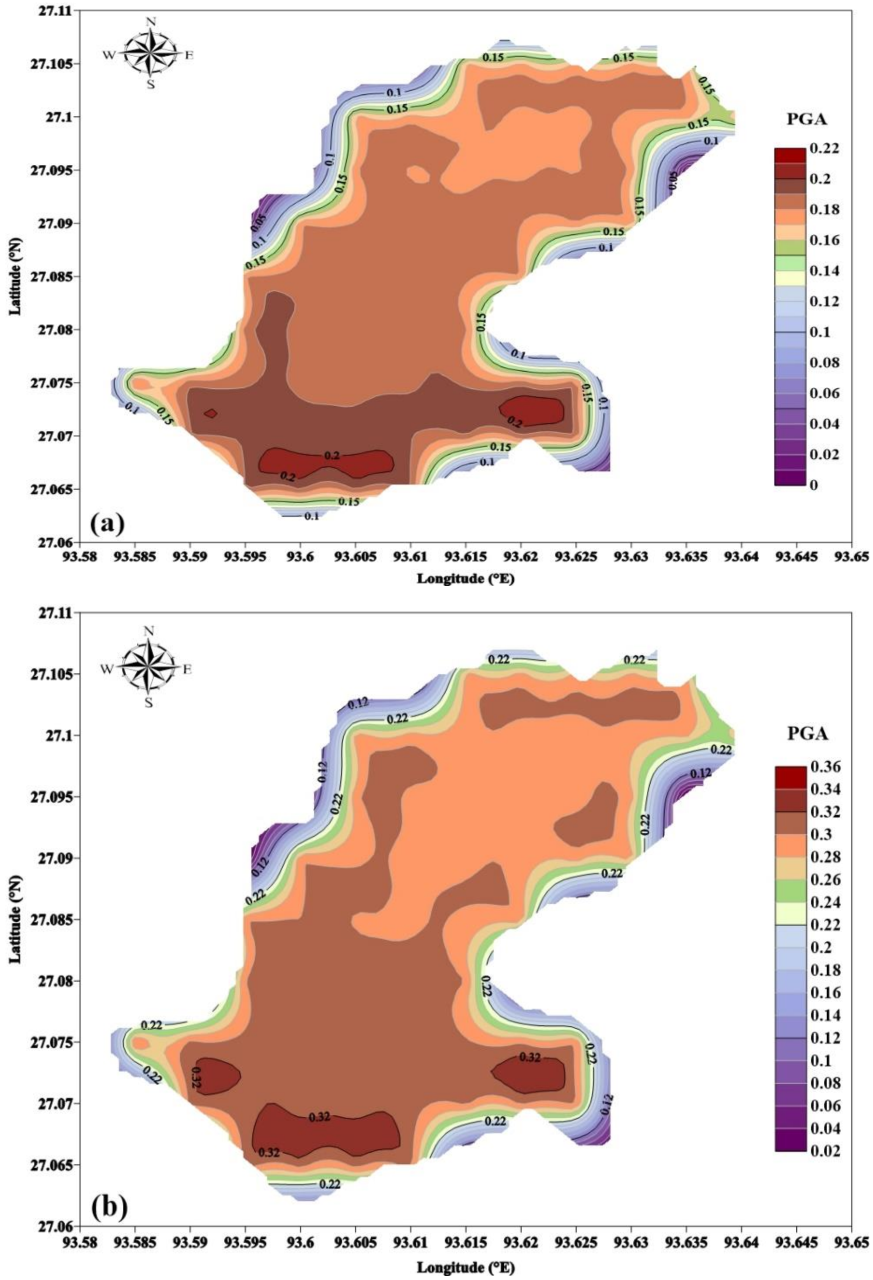

Fig. 7 PHA map of Itanagar for (a) 10% probability of exceedance in 50 years for return period of 475 years (b) 2% probability of exceedance in 50 years for return period of 2475 years

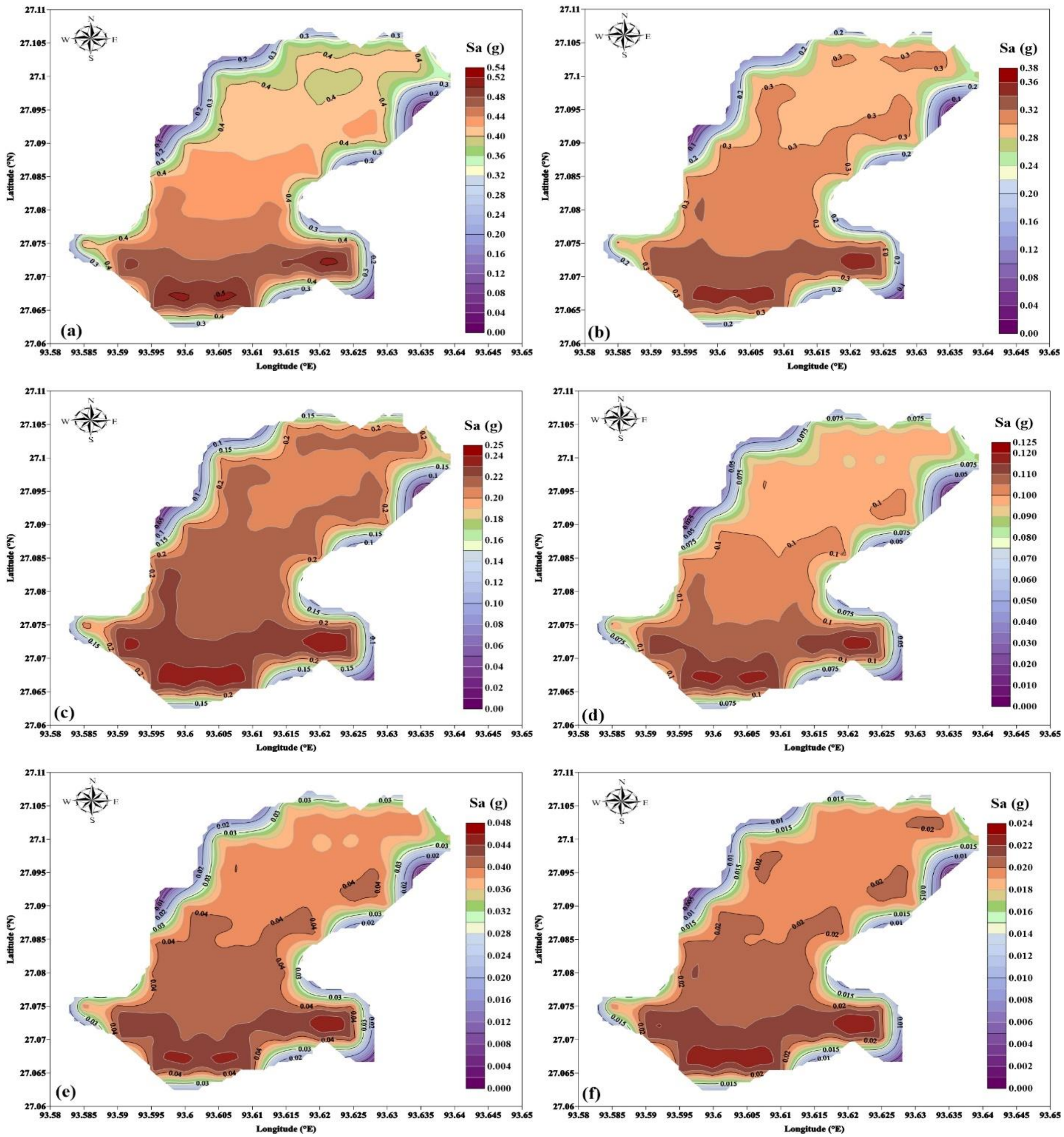

Fig. 8 Spectral acceleration in g at periods of (a) 0.1 s (b) 0.3 s (c) 0.5 s (d) 1.0 s (e) 2.0 s (f) 3.0 s, for a 475 year return period

The spectral acceleration contours for the study region, at return periods of 2475 year, at periods of 0.1 s, 0.3 s, 0.5 s, 1.0 s, 2.0 s and 3.0 s, is presented as contour plots in Fig. 9(a-f). The results indicate that the southern and central regions exhibit consistently higher S_a values across all periods, suggesting these areas are more susceptible to severe ground motion during earthquakes.

At the shortest spectral period (0.1 s), S_a values reach a maximum of 0.95g in the southern region, reflecting high seismic intensity likely due to local soil amplification and tectonic activity. Conversely, the northern and western regions demonstrate relatively lower S_a values, with ranges of 0.20g to 0.35g at 0.1 s, gradually decreasing to 0.02g to 0.04g at 3.0 s, indicating lower seismic hazard in these areas.

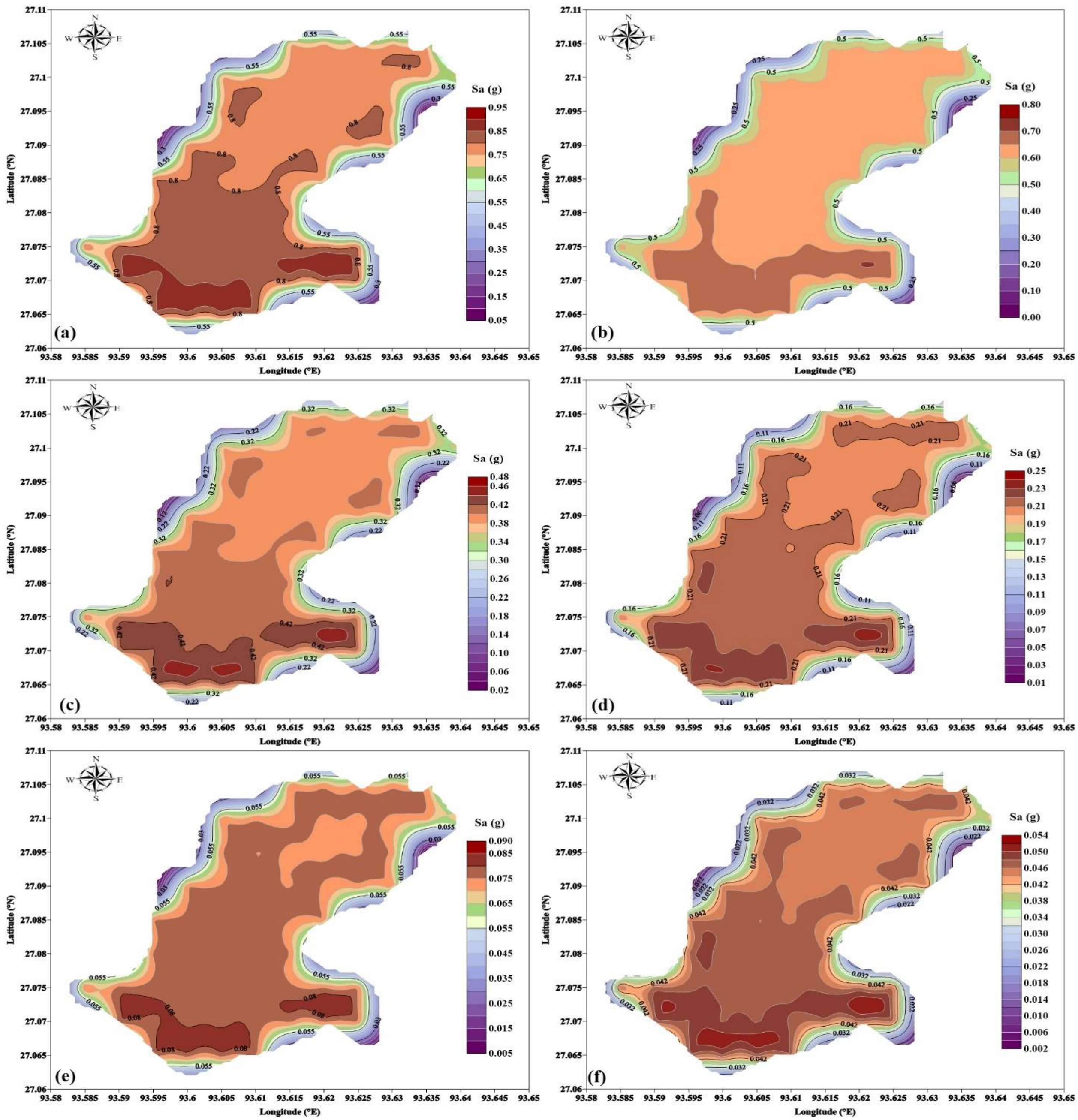

Fig. 9 Spectral acceleration in g at periods of (a) 0.1 s (b) 0.3 s (c) 0.5 s (d) 1.0 s (e) 2.0 s (f) 3.0 s, for a 2475 year return period

Table 6. Comparison of PHA values from the present study with previous studies for Northeast India

References	PHA (g) for 10% in 50 years exceedance
Bhatia *et al*. [93]	0.25-0.45
Das *et al*. [92]	0.18–0.22
IS-1893 [38]	0.18
Sharma and Malik [94]	0.3-0.48
Desai and Choudhury [31]	0.095-0.2
NDMA [66]	0.15-0.35
Nath and Thingbaijam [95]	0.5-1.12
Pallav *et al*. [51]	0.13-0.19
Borgohain *et al*. [38]	0.59
Bahuguna and Sil [37]	0.2-0.48
Kumar *et al*. [96]	0.25
Shukla and Choudhury [28]	0.23-0.34
Present Study	0.22

As the spectral period increases, S_a values decrease across all regions, with the highest values at 3.0 s remaining in the central and southern areas, peaking at 0.08g-0.09g. The central region consistently exhibits moderate to high S_a values across all periods, highlighting it as a critical area for seismic design considerations. The seismic hazard map for both the return period shows uniform hazard inside the zones and sharp changes in hazard values at their edges. The observed decrease in S_a values with increasing spectral periods reflects the attenuation of seismic energy over time, a trend consistent with established seismic hazard principles. This analysis underscores the importance of incorporating spatially resolved spectral acceleration data into the seismic design of infrastructure and urban planning to mitigate earthquake risks effectively. The findings of the current study are compared with the results of other researchers, focusing on the return period of 475 years. A detailed comparison is presented in Table 6, highlighting the similarities and differences in PHA values. The present study reports a PHA value of 0.22g for 10% probability of exceedance in 50 years for return period of 475 years, which aligns closely with findings from similar studies. Das *et al*. [92] provides a range of 0.18–0.22g, overlapping entirely with the present study, indicating consistent seismic hazard levels. IS-1893 specifies a value of 0.18g, which is slightly lower than the values obtained in the present study, reflecting the typically conservative estimates adopted in building codes [38]. Similarly, NDMA [66], reported values ranging from

0.15g to 0.35g; the values obtained from the present study are found to lie near the lower to mid-range of this bound. However, Pallav *et al*. [51] reported values between 0.13g and 0.19g, notably lower than the findings of the present study. Overall, the present study's estimate is consistent with prior research, reflecting a moderate seismic hazard assessment that is slightly higher than some conservative estimates but lower than broader regional assessments.

8. Summary and Conclusions

This study explores the seismic hazard of Itanagar city, located in the state of Arunachal Pradesh in Northeast India, using a probabilistic analysis approach. The analysis considers 18 fault lines that contribute to ground motion within and around the study region. The output consists of PHA and spectral acceleration (S_a) values for different return periods, aiding in seismic hazard assessment and infrastructure design for the region. This study uses an earthquake catalogue from 1900-2024, consisting of 2054 mainshock events, to understand earthquake phenomena in the region. Declustering is used to remove foreshocks and aftershocks, and the completeness of the catalogue is examined using the CUVI method. Characterization of earthquake sources involves developing tectonic maps, identifying all sources that can cause damaging earthquakes, measuring fault lengths, determining the magnitude of the most damaging earthquakes observed, and estimating the magnitude potential of seismogenic sources. The Geological Survey of India developed SEISAT to analyze seismic activity in India. A 500 km radius around Itanagar is examined using high-resolution scans of sheets 13-17, and a tectonic map is created. 33 active tectonic features are identified, and 18 major active tectonic features capable of producing significant ground motion were selected for seismic hazard analysis. Based on the present study, the following conclusions are drawn:

- The *b*-value of Itanagar city ranges between 0.68±0.04 to 0.89±0.03. These values reflect the stress regime and tectonic complexity of the region.
- The GMPE proposed by Boore *et al*. [86] is identified as the most suitable model for the region, enabling precise calculation of seismic hazard parameters. PHA values were determined as 0.22g for a 2% probability of exceedance and 0.36g for a 10% probability of exceedance, both within a 50-year timeframe.
- The spectral accelerations were computed for two return periods 475 and 2475 years at specific time periods of 0.1 s, 0.3 s, 0.5 s, 1.0 s, 2.0 s, and 3.0 s. For the 475 year return

period, the spectral acceleration values are 0.54g, 0.38g, 0.25g, 0.125g, 0.048g, and 0.024 g, respectively. For the 2475 year return period, the corresponding spectral accelerations are 0.95g, 0.80g, 0.48g, 0.250g, 0.09g, and 0.054g, respectively.

The results of the seismic hazard study will provide the necessary data to accurately identify and map the seismically active zones, assess the seismic hazard, and determine the seismic intensity levels in the area. This data can then be used to make informed decisions about seismic-resistant design of structures, as well as seismic zonation studies, to ensure that structures are adequately protected from seismic hazards. Further, future studies can be undertaken to improve magnitude conversion methods by developing region-specific magnitude conversion equations for the study area. Moreover, attempts should be made to detailed geological data, rupture lengths, and fault displacement characteristics to produce more accurate seismic hazard assessments. Additionally, the development of region-specific Ground Motion Prediction Equations (GMPEs) to achieve precise ground-motion predictions and enable comparisons with global models for the Itangar region should be one of the prime focus of future studies.

Funding

The authors thank the Arunachal Pradesh Public Work Department for funding the project ‘‘Seismic microzonation of Itanagar region’’ (Ref.No. CE/P/JT/02/2022/PWD).

Compliance with Ethical Standards

Conflict of Interest: The authors declare that they have no known competing financial interests or personal relationships that could have appeared to influence the work reported in this paper.

Ethical Approval: This article does not contain any studies with human participants or animals performed by any of the authors.

Informed Consent: For this type of study, formal consent is not required.

Author Contributions: AKA: Conceptualization, Formal analysis, Writing–Original preparation; **JT:** Supervision, Formal analysis, Revision and Editing of drafted manuscript; **SSK & AD:** Conceptualization, Revision and Editing of drafted manuscript

Reference

1. Ansal, A. (2004). Recent Advances in Earthquake Geotechnical Engineering and Microzonation. Springer. https://doi.org/10.1007/1-4020-2528-9
2. Anshu AK, Taipodia J, Kumar SS, Dey A (2024) Identification of ground response parameters of Itanagar city, Arunachal Pradesh, India, using varying seismic intensities and equivalent linear analysis approach. Indian Geotech J 1–23. http://dx.doi.org/10.1007/s40098-024-00967-w
3. Kumar SS, Krishna AM, Dey A (2018) Dynamic properties and liquefaction behaviour of cohesive soil in Northeast India under staged cyclic loading. J Rock Mech Geotech Eng 10(5):958–967. https://doi.org/10.1016/j.jrmge.2018.04.004
4. Kumar SS, Dey A, Krishna AM (2020) Liquefaction potential assessment of Brahmaputra sand based on regular and irregular excitations using stress-controlled cyclic triaxial test. KSCE J Civ Eng 24(4):1070–1082. https://doi.org/10.1007/s12205-020-0216-x
5. Kumar SS, Dey A, Krishna AM (2018) Response of saturated cohesionless soil subjected to irregular seismic excitations. Nat Hazards 93:509–529. https://link.springer.com/article/10.1007/s11069-018-3312-1
6. Kumar SS, Dey A, Krishna AM (2018) Importance of site-specific dynamic soil properties for seismic ground response studies: ground response analysis. Int J Geotech Earthq Eng 9(1):78–98. http://dx.doi.org/10.4018/IJGEE.2018010105
7. Ridwan M, Widiyantoro S, Irsyam M, Faizal L, Cummins PR, Rawlinson N, Goro GL (2024) Seismic microzonation of Bandung, West Java: Site characterization and its implications for seismic hazard. Nat Hazards 1–16. http://dx.doi.org/10.1007/s11069-024-07010-4
8. Puri N, Jain A (2016) Deterministic seismic hazard analysis for the state of Haryana, India. Indian Geotech J 46:164–174. https://doi.org/10.1007/s40098-015-0167-1
9. Puri N, Jain A (2018) Possible seismic hazards in Chandigarh City of North-western India due to its proximity to Himalayan frontal thrust. J Ind Geophys Union 22(5):485–506.
10. Kumar A, Kotoky N, Shekhar S (2024) Spatial variation of seismicity parameters in Meghalaya, North-East India. Acta Geophysica 1–19. http://dx.doi.org/10.1007/s11600-024-01290-x
11. Satyannarayana R, Rajesh BG (2021) Seismotectonic map and seismicity parameters for Amaravati area, India. Arabian J Geosciences 14:1–24. https://doi.org/10.1007/s12517-021-08622-x
12. Kumar A, Haldar S (2020) Design response spectra and site coefficients for various seismic site classes of Guwahati, India, based on extensive ground response analyses. Geotech Geol Eng. https://link.springer.com/article/10.1007/s10706-020-01434-y
13. Baruwal R, Chhetri B, Chaulagain H (2020) Probabilistic seismic hazard analysis and construction of design spectra for Pokhara Valley, Nepal. Asian J Civil Eng 21(8):1297–1308. https://link.springer.com/article/10.1007/s42107-020-00278-4

14. Joshi R, Sudhir SB and Suresh SK (2020) Probabilistic seismic hazard analysis of Madhya Pradesh (Central India) using alternate source models: A logic tree approach. Asian J Civil Eng 21:1399-1414. https://doi.org/10.1007/s42107-020-00286-4.

15. Mehta P, Thaker TP (2020) Seismic hazard analysis of Vadodara region, Gujarat, India: Probabilistic and deterministic approach. J Earthq Eng. 26(3):1438-1460. https://doi.org/10.1080/13632469.2020.1724212

16. Sandhu M, Sharma B, Mittal H, Prasantha C (2020) Analysis of the site effects in the north east region of India using the recorded strong ground motions from moderate earthquakes. J Earthq Eng. 26(3):1480-1499. https://doi.org/10.1080/13632469.2020.1724214

17. Khan MM, Teja M, Kiran NN, Kumar GK (2020) Seismic hazard curves for Warangal city in peninsular India. Asian J Civil Eng 21(3):543–554. https://link.springer.com/article/10.1007/s42107-019-00210-5

18. Naik N, Choudhury D (2015) Deterministic seismic hazard analysis considering different seismicity levels for the state of Goa, India. Nat Hazards 75(1):557–580. http://dx.doi.org/10.1007/s11069-014-1346-6

19. Anbazhagan P, Bajaj K, Patel S (2015) Seismic hazard maps and spectrum for Patna considering region-specific seismotectonic parameters. Nat Hazards, 78:1163-1195. http://dx.doi.org/10.1007/s11069-015-1764-0

20. Kataria NP, Shrikhande M, Das JD (2013) Deterministic seismic hazard analysis of Andaman and Nicobar Islands. J Earthq Tsunami 07(04). https://doi.org/10.1142/S1793431113500358

21. Thaker TP, Ganesh WR, Rao KS, Gupta KK (2012) Use of seismotectonic information for the seismic hazard analysis for Surat City, Gujarat, India: Deterministic and probabilistic approach. Pure Appl Geophys 169(1–2):37–54. https://doi.org/10.1007/s00024-011-0317-z

22. Chopra S, Kumar D, Rastogi BK, Choudhury P, Yadav RBS (2012) Deterministic seismic scenario for Gujarat region, India. Nat Hazards 60:517–540. http://dx.doi.org/10.1007/s11069-011-0027-y

23. Kolathayar S, Sitharam TG, Vipin KS (2012) Deterministic seismic hazard macrozonation of India. J Earth Syst Sci 121(5):1351–1364. http://dx.doi.org/10.1007/s12040-012-0227-1

24. Mahajan AK, Thakur VC, Sharma ML, Chauhan M (2010) Probabilistic seismic hazard map of NW Himalaya and its adjoining area, India. Nat Hazards 53(3):443–457. http://dx.doi.org/10.1007/s11069-009-9439-3

25. Shanker D, Sharma ML (1998) Estimation of seismic hazard parameters for the Himalayas and its vicinity from complete data files. Pure Appl Geophys 152:267–279. https://doi.org/10.1007/s000240050154

26. Iyengar RN, Ghosh S (2004) Microzonation of earthquake hazard in greater Delhi area. Curr Sci 87(9):1193–1202.

27. Anbazhagan P, Vinod J, Sitharam T (2009) Probabilistic seismic hazard analysis for Bangalore. Nat Hazards 48:145–166. https://doi.org/10.1007/S11069-008-9253-3

28. Shukla J, Choudhury D (2012) Estimation of probabilistic seismic hazard and site-specific ground motions for two ports in Gujarat. In GeoCongress 2012: State of the Art and Practice in Geotechnical Engineering, 1650-1659. http://dx.doi.org/10.1061/9780784412121.170

29. Mohanty W, Verma A (2013) Probabilistic seismic hazard analysis for Kakrapar atomic power station, Gujarat, India. Nat Hazards 69:919–952. https://doi.org/10.1007/s11069-013-0744-5

30. Ashish, Lindholm C, Parvez IA, Kühn D (2016) Probabilistic earthquake hazard assessment for Peninsular India. J Seismol 20:629–653. https://link.springer.com/article/10.1007/s10950-015-9548-2

31. Desai SS, Choudhury D (2014) Spatial variation of probabilistic seismic hazard for Mumbai and surrounding region. Nat Hazards 71:1873–1898. https://doi.org/10.1007/s11069-013-0984-4

32. IS-1893 (2016) Indian standard criteria for earthquake resistant design of structures, Part-I, General provisions and buildings, Bureau of Indian standard, New Delhi.

33. Patil S, Menon A, Dodagoudar G (2018) Probabilistic seismic hazard at the archaeological site of Gol Gumbaz in Vijayapura, south India. J Earth Syst Sci 127:1–24. https://doi.org/10.1007/s12040-018-0917-4

34. Shukla D, Solanki CH (2021) Probabilistic seismic hazard assessment for Indore city and surrounding areas. Innov Infrastruct Solut 6(3):138. https://doi.org/10.1007/s41062-021-00456-6

35. Das R, Sharma M, Wason H (2016) Probabilistic seismic hazard assessment for Northeast India region. Pure Appl Geophys 173:2653–2670. https://doi.org/10.1007/s00024-016-1333-9

36. Sil A, Sitharam T, Kolathayar S (2013) Probabilistic seismic hazard analysis of Tripura and Mizoram states. Nat Hazards 68:1089–1108. https://doi.org/10.1007/s11069-013-0678-y

37. Bahuguna A, Sil A (2020) Comprehensive seismicity, seismic sources, and seismic hazard assessment of Assam, Northeast India. J Earthq Eng 24(2):254–297. http://dx.doi.org/10.1080/13632469.2018.1453405v

38. Borgohain H, Baruah S, Sharma S (2024) Site characterisation and probabilistic seismic hazard assessment in Tura City, Meghalaya. J Earth Syst Sci 133(2):1–18. http://dx.doi.org/10.1007/s12040-024-02291-6

39. Maiti SK, Nath SK, Adhikari MD, Srivastava N, Sengupta P, Gupta AK (2016) Probabilistic seismic hazard model of West Bengal, India. J Earthq Eng 21(7):1113–1157. https://doi.org/10.1080/13632469.2016.1210054

40. Patnaik SK (2021) Urban housing in Itanagar: Mountain geomorphology and hazard vulnerability vis-a-vis smart city framework. In: Geospatial Technology and Smart Cities: ICT, Geoscience Modeling, GIS and Remote Sensing, pp 381–401.

41. Chen WP, Molnar P (1990) Source parameters of earthquakes and intraplate deformation beneath the Shillong Plateau and northern Indo-Burma ranges. J Geophys Res 95:12527–12552. https://doi.org/10.1029/JB095iB08p12527

42. Nandy DR (2001) Geodynamics of Northeastern India and adjoining regions. ACB Publication, Kolkata, pp 209.

43. Kayal JR (2008) Microearthquake seismology and seismotectonics of Southeast Asia. Capital Publishing Company, New Delhi, pp 503.

44. Verma RK, Mukhopadhyay M (1977) An analysis of the gravity field in Northeast India. Tectonophysics 42:283–317. https://doi.org/10.1016/0040-1951(77)90171-8

45. Khattri KN, Tyagi AK (1983) Seismicity patterns in the Himalayan plate boundary and identification of the areas of high seismic potential. Tectonophysics 96:281–297. https://doi.org/10.1016/0040-1951%2883%2990222-6

46. Kayal JR (2001) Microearthquake activity in some parts of the Himalaya and the tectonic model. Tectonophysics 339:331–333. http://dx.doi.org/10.1016/S0040-1951(01)00129-9

47. Kayal JR (1987) Microseismicity and source mechanism study: Shillong Plateau, Northeast India. Bull Seismol Soc Am 77:184–194. http://dx.doi.org/10.1785/BSSA0770010184

48. Khattri KN, Wyss M (1979) Precursory variation of seismic rate in Assam Area, India. Mausam 6:685–688. https://doi.org/10.54302/mausam.v30i2.3038

49. Molnar P, Tapponnier P (1977) Relation of the tectonics of Eastern China to the India-Eurasia collision: Application of slip-line field theory to large-scale control tectonics. Geology 5:212–216. https://doi.org/10.1130/0091-7613(1977)5%3C212:ROTTOE%3E2.0.CO;2

50. Gansser A (1974) The Ophiolitic Mélange: A worldwide problem on Tethyan examples. Eclogae Geol Helv 67:479–507.

51. Pallav K, Raghukanth STG, Singh KD (2012) Probabilistic seismic hazard estimation of Manipur, India. J Geophys Eng 9(5):516–533. https://doi.org/10.1088/1742-2132/9/5/516

52. Scordilis EM (2006) Empirical global relations converting M_s and M_b to moment magnitude. J Seismol 10:225–236. http://dx.doi.org/10.1007/s10950-006-9012-4

53. Kolathayar S, Sitharam TG, Vipin KS (2012) Spatial variation of seismicity parameters across India and adjoining areas. Nat Hazards 60:1365–1379. http://dx.doi.org/10.1007/s11069-011-9898-1

54. Gardner JK, Knopoff L (1974) Is the sequence of earthquakes in Southern California with aftershocks removed, Poissonian? Bull Seismol Soc Am 64(5):1363–1367.

55. Reasenberg P (1985) Second-order moment of central California seismicity, 1969–1982. J Geophys Res Solid Earth 90(B7):5479–5495. https://doi.org/10.1029/JB090iB07p05479

56. Davis SD, Frohlich C (1991) Single-link cluster analysis, synthetic earthquake catalogs, and aftershock identification. Geophys J Int 104:289–306. https://doi.org/10.1111/j.1365-246X.1991.tb02512.x

57. Molchan G, Dmitrieva O (1992) Aftershock identification: Methods and new approaches. Geophys J Int 109:501–516. http://dx.doi.org/10.1111/j.1365-246X.1992.tb00113.x

58. Wiemer S (2001) A software package to analyze seismicity: ZMAP. Seismol Res Lett 72(3):373–382. http://dx.doi.org/10.1785/gssrl.72.3.373

59. Tinti S, Mulargia F (1985) Completeness analysis of a seismic catalog. Ann Geophys 3(3):407–414.

60. Dasgupta S, Pande P, Ganguly D, Iqbal Z, Sanyal K, Venkataraman NV, Sural B, Harendranath L, Mazumdar K, Sanyal S, Roy A (2000) Seismotectonic Atlas of India and its environs. Spec Publ Geol Surv India, Calcutta, 86 p.

61. Puri N, Jain A (2019) Microzonation of seismic hazard for the state of Haryana, India. J Geol Soc India 94:297–308. https://doi.org/10.1007/s12594-019-1310-x

62. Wells DL, Coppersmith KJ (1994) New empirical relationships among magnitude, rupture length, rupture width, rupture area, and surface displacement. Bull Seismol Soc Am 84:974–1002. https://doi.org/10.17660/actahortic.2012.930.15

63. Gupta ID (2002) The state of the art in seismic hazard analysis. ISET J Earthq Technol 39:311–346.

64. Kijko A (2004) Estimation of the maximum earthquake magnitude, M_{max}. Pure Appl Geophys 161:1655–1681. https://doi.org/10.1007/s00024-004-2531-4

65. Mueller CS (2010) The influence of maximum magnitude on seismic hazard estimates in the Central and Eastern United States. Bull Seismol Soc Am 100:699–711. https://doi.org/10.1785/0120090114

66. NDMA (2010) Development of probabilistic seismic hazard map of India. Technical report, National Disaster Management Authority, Government of India, New Delhi.

67. Sitharam TG, Sil A (2014) Comprehensive seismic hazard assessment of Tripura and Mizoram states. J Earth Syst Sci 123:837–857. https://doi.org/10.1007/s12040-014-0438-8

68. Anbazhagan P, Vinod JS, Sitharam TG (2007) Probabilistic seismic hazard analysis with local site effects. In: A Workshop on Microzonation, 122–138.

69. Gutenberg B, Richter CF (1954) Seismicity of the earth and associated phenomena. Princeton University Press, Princeton, NJ, USA.

70. Merz HA, Cornell CA (1973) Seismic risk analysis based on a quadratic magnitude-frequency law. Bull Seismol Soc Am 63(6-1):1999–2006. https://doi.org/10.1785/BSSA0636-11999

71. Jaiswal K, Sinha R (2006) Probabilistic modeling of earthquake hazard in stable continental shield of the Indian Peninsula. ISET J Earthq Technol 43(3):49–64.

72. Ram A, Rathor HS (1970) On frequency magnitude and energy of significant Indian earthquakes. Pure Appl Geophys 79:26–32. https://doi.org/10.1007/BF00875475

73. Kaila KL, Gaur VK, Narain Hari (1972) Quantitative seismicity maps of India. Bull Seismol Soc Am 62:1119–1131. https://doi.org/10.1785/BSSA0620051119

74. Rao BR, Rao PS (1984) Historical seismicity of Peninsular India. Bull Seismol Soc Am 74:2519–2533. https://doi.org/10.1785/BSSA0740062519

75. Raghukanth, S. T. G., Iyengar, R. N. (2006) Seismic hazard estimation for Mumbai city. Current Science, 1486-1494

76. Vipin, K S, Anbazhagan P, Sitharam T G (2009) Estimation of peak ground acceleration and spectral acceleration for South India with local site effects: probabilistic approach. Nat Haz and Earth Sys Sci 9(3): 865-878. https://doi.org/10.5194/nhess-9-865-2009

77. Menon A, Ornthammarath T, Corigliano M, Lai C G (2010) Probabilistic seismic hazard macrozonation of Tamil Nadu in Southern India. Bulletin of the Seismological Society of America 100(3):1320-1341. https://doi.org/10.1785/0120090071

78. Sitharam T G, James N, Vipin K S, Raj K G (2012) A study on seismicity and seismic hazard for Karnataka State. J of Earth Sys Sci 121:475-490. https://doi.org/10.1007/s12040-012-0171-0

79. Shukla J, Choudhury D (2012) Estimation of seismic ground motions using deterministic approach for major cities of Gujarat. Nat Haz and Earth Sys Sci 12(6):2019-2037. https://doi.org/10.5194/nhess-12-2019-2012

80. Kumar A, Anbazhagan P, Sitharam T G (2013) Seismic hazard analysis of Lucknow considering local and active seismic gaps. Nat hazards 69:327-350. https://doi.org/10.1007/s11069-013-0712-0

81. Naik N, Choudhury D (2014) Development of fault and seismicity maps for the state of Goa, India. Disaster Advances 7(6): 12-24.

82. Shiuly A, Sahu R B and Mandal S (2015) Seismic microzonation of Kolkata Geomech. Eng. 9 125–44.

83. Ordaz M, Salgado-Gálvez MA (2017) R-Crisis validation and verification document. Technical report, Mexico City, Mexico.

84. Nath SK, Thingbaijam KK (2010) Peak ground motion predictions in India: an appraisal for rock sites. J Seismol 15:295–315. http://dx.doi.org/10.1007/s10950-010-9224-5

85. Douglas J (2022) Ground motion prediction equations 1964–2014. University of Strathclyde, Glasgow, UK.

86. Boore DM, Stewart JP, Seyhan E, Atkinson GM (2014) NGA-West2 equations for predicting PGA, PGV, and 5% damped PSA for shallow crustal earthquakes. Earthq Spectra 30(3):1057–1085. http://dx.doi.org/10.1193/070113EQS184M

87. Rahman M Z, Siddiqua S, Kamal A M (2020) Seismic source modeling and probabilistic seismic hazard analysis for Bangladesh. Nat Hazards 103:2489-2532. https://doi.org/10.1007/s11069-020-04094-6

88. Sharma S, Mannu U, Singh Bora S (2024) Epistemic uncertainty in ground-motion characterization in the Indian context: Evaluation of ground-motion models (GMMs) for the Himalayan region. Seismol Res Lett, 95(3), 1718-1734. https://doi.org/10.1785/0220230157

89. Ornthammarath T, Warnitchai P, Chan CH, Wang Y, Shi X, Nguyen PH, Nguyen LM, Kosuwan S, Thant M (2020) Probabilistic seismic hazard assessments for Northern Southeast Asia (Indochina): Smooth seismicity approach. Earthq Spectra 36(1_suppl): 69-90. https://doi.org/10.1177/8755293020942528

90. Ghione F, Poggi V, Lindholm C (2021) A hybrid probabilistic seismic hazard model for Northeast India and Bhutan combining distributed seismicity and finite faults. Phys. Chem. Earth, Parts A/B/C, 123, 103029. https://doi.org/10.1016/j.pce.2021.103029

91. Lallawmawma C, Sharma M L, Das J (2022) Probabilistic seismic hazard assessment of North East India. Symp Earthq Eng Singapore: Springer Nature Singapore 187-204. https://doi.org/10.1007/978-981-99-1459-3_16

92. Das S, Gupta ID, Gupta VK (2006) A probabilistic seismic hazard analysis of Northeast India. Earthq Spectra 22(1):1–27. http://dx.doi.org/10.1193/1.2163914

93. Bhatia SC, Ravi Kumar M, Gupta HK (1999) A probabilistic seismic hazard map of India and adjoining regions. Ann Geophys 42(6):1153–1166. http://dx.doi.org/10.4401/ag-3777

94. Sharma ML, Malik S (2006) Probabilistic seismic hazard analysis and estimation of spectral strong ground motion on bedrock in Northeast India. 4th Int Conf Earthq Eng, Taipei, Taiwan.

95. Nath SK, Thingbaijam KK (2012) Probabilistic seismic hazard assessment of India. Seismol Res Lett 83(1):135–149. http://dx.doi.org/10.1785/gssrl.83.1.135

96. Kumar A, Ghosh G, Gupta PK, Kumar V, Paramasivam P (2023) Seismic hazard analysis of Silchar city located in Northeast India. Geomatics Nat Hazards Risk 14(1):2170831. https://doi.org/10.1080/19475705.2023.2170831